DAMAGE TENSORS AND THE CRACK DENSITY DISTRIBUTION

V. A. LUBARDA and D. KRAJCINOVIC

Department of Mechanical and Aerospace Engineering, Arizona State University,
Tempe, AZ 85287-6106, U.S.A.

Abstract—The paper presents an algorithm for the derivation of damage tensors emphasizing its relationship with the actual and approximate crack density distributions. The proposed model is illustrated using scalar, second and fourth order continuous tensor approximations of some typical two and three dimensional crack distributions. It is also shown that the occurrence of regions with negative crack density (anticrack regions) is in many cases a common and as yet unexplored feature of the approximate solutions.

1. INTRODUCTION

Brittle deformation processes in materials with inferior tensile strength, such as rocks, concrete, ceramics and some glassy polymers, are of continuing interest for practitioners and theorists alike. In a great majority of cases the inelastic deformation of these materials is, at room temperature, attributable to microcracking. Some of the early continuum damage theories made an attempt to model the macro response of brittle processes modifying existing plasticity theory. However, the constraints which are placed by microcracks on the displacement field are radically different from those imposed by crystalline slips. The difference between brittle and ductile deformation is further emphasized by the fact that the microcrack growth in a fundamental manner depends on the sign of normal stresses. It is, therefore, not surprising that the plasticity based phenomenological models were not particularly successful in replicating salient aspects of the brittle deformation caused by nucleation and growth of a large number of microcracks.

The rapid development of the continuum damage mechanics in the last two decades produced various contrasting and even contradictory phenomenological models. Using clever artifices various authors suggested a host of different mathematical representations for the damage (internal, hidden) variable. The list runs from scalars (Kachanov, 1958; Lemaitre and Chaboche, 1978; Lemaitre, 1987; etc.), axial vectors (Davison and Stevens, 1973; Krajcinovic and Fonseka, 1981; Talreja, 1985; etc.), second order tensors (Vakulenko and Kachanov, 1971; Dragon and Mroz, 1979; Kachanov, 1980, 1992; Cordebois and Sidoroff, 1982; Murakami, 1988; Karihaloo and Fu, 1989; etc.), fourth order tensors (Chaboche, 1982; Simo and Ju, 1987; Chow and Wang, 1988; Krajcinovic, 1989; Lubarda and Krajcinovic, 1993; etc.), to a series containing all even order tensors (Onat and Leckie, 1988).

The primary objective of this paper is to examine the relationship between a given, experimentally determined, distribution of cracks and the scalar, second order and fourth order tensor damage parameters. The experimentally measured microcrack densities in planes with different inclinations are typically represented in form of the rosette histogram. This rosette histogram is subsequently approximated by a distribution function defined on a unit sphere and centered in a material point. This distribution function can be further expanded into a series of spherical functions containing dyadic products of unit vectors and the Kronecker delta tensor. The ensuing series is typically truncated at a desired tensorial rank of these dyadic products. In this sense each of the above mentioned damage representations is an approximation which may or may not be sufficiently accurate in each particular case. The objective of this study is to present an algorithm for the derivation of the damage parameters and to examine their ability to approximate the microcrack distribution function in several important cases. A common feature that occurs in many cases, when

either second or fourth order damage tensors are utilized to approximate the actual crack distribution, are the regions of negative crack density.

2. DAMAGE TENSORS AND THE CRACK DENSITY DISTRIBUTION

Consider a solid specimen containing a certain distribution of microcracks accumulated during a specific loading program from some initial state. Various damage variables were introduced in the literature to adequately represent the degraded state of the material. If the current crack pattern in the representative volume element is such that cracks are uniformly distributed in all planes, regardless of their orientation, a scalar damage variable becomes a natural choice. The corresponding distribution of damage is referred to as isotropic. If cracks are nonuniformly distributed over differently oriented planes, the damage distribution and correspondingly the material response are anisotropic. A distribution function $\rho(\mathbf{n})$ (defined on a unit sphere) must in this case be introduced to define the directional dependence of the crack density. This function can be expanded in a Fourier-type series of certain families of spherical functions (Kanatani, 1984; Onat and Leckie, 1988), containing dyadic products of the unit vector and the Kronecker delta tensor. In addition to the scalar (isotropic) term, the second, fourth and higher even order symmetric tensors appear in this representation. Therefore, the accurate analytical description of damage by even higher order tensors is a complicated task, which has generated a lot of controversy in the last two decades. The following derivation in Section 2 is based on more general development, presented by Kanatani (1984).

2.1. Scalar damage variable

If the crack distribution is isotropic, the crack density does not depend on the orientation of the normal $\mathbf{n}$ to the plane through a material point, i.e.:

$$\rho(\mathbf{n}) = \rho. \tag{1}$$

Expression (1) can also be used to approximate a nearly isotropic distribution, in which case $\rho(\mathbf{n})$ is not a constant, but varies weakly with the orientation of the unit vector $\mathbf{n}$. The value of the average crack density ρ is then obtained by integrating eqn (1) over all directions spanning the entire solid angle $\Omega = 4\pi$

$$\int_{4\pi} \rho(\mathbf{n}) \, d\Omega = 4\pi\rho. \tag{2}$$

From eqn (2) the average crack density is:

$$\rho = \frac{\rho_0}{4\pi}, \tag{3}$$

where

$$\rho_0 = \int_{4\pi} \rho(\mathbf{n}) \, d\Omega, \tag{4}$$

is the density of all cracks within a representative unit volume. Consequently, the damage is characterized by a single scalar parameter ρ_0, which does not change the existing symmetries of the original matrix. As a result of its simplicity, the scalar damage variable was extensively utilized in the literature (Lemaitre, 1987, 1992).

2.2. Second order damage tensor

In a general case of loading of initially anisotropic rocks the planes containing extreme densities of damage are not mutually perpendicular. Consequently, both the damage itself and its effect on the material effective stiffness are anisotropic. However, in the case of

initially isotropic materials subjected to proportional loading, the density of damage is maximum in the plane perpendicular to the largest principal stress, and minimum in the plane normal to the minimum principal stress. To study this case of damage distribution, it seems reasonable to approximate its density distribution by an oval curve (Fig. 1). This class of damage distribution can be approximated adequately by a second order tensor. If ρ_{ij} denotes the components of the second order crack density tensor, the density of cracks embedded in the planes with a normal $\mathbf{n}$ is defined by the expression:

$$\rho(\mathbf{n}) = \rho_{kl}n_k n_l, \tag{5}$$

depicted by the oval shape of Fig. 1. Integrating eqn (5) over the entire solid angle, and using:

$$\int_{4\pi} n_i n_j \, d\Omega = \frac{4\pi}{3}\delta_{ij}, \tag{6}$$

where δ_{ij} denotes the Kronecker delta tensor, it follows that the first invariant of the second order crack density tensor is:

$$\rho_{kk} = \frac{3\rho_0}{4\pi}. \tag{7}$$

The summation convention is used for the repeated indices, and ρ_0 is the total crack density, defined by eqn (4).

Multiplying eqn (5) with $n_i n_j$, integrating over all directions and using:

$$\int_{4\pi} n_i n_j n_k n_l \, d\Omega = \frac{4\pi}{5} I_{ijkl}, \tag{8}$$

it follows that:

$$\frac{8\pi}{15}\left(\rho_{ij} + \frac{1}{2}\rho_{kk}\delta_{ij}\right) = \int_{4\pi} \rho(\mathbf{n})n_i n_j \, d\Omega. \tag{9}$$

In eqn (8)

$$I_{ijkl} = \tfrac{1}{3}(\delta_{ij}\delta_{kl} + \delta_{ik}\delta_{jl} + \delta_{il}\delta_{jk}). \tag{10}$$

Substituting eqn (7) into eqn (9), the crack density tensor can be expressed as:

$$\rho_{ij} = \frac{15}{8\pi}\left(D_{ij} - \frac{\rho_0}{5}\delta_{ij}\right). \tag{11}$$
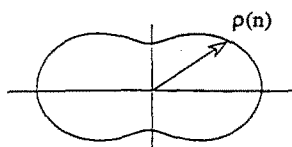
The symmetric second order tensor:

Fig. 1. An oval shape corresponding to the second order tensor description of the crack density distribution.

$$D_{ij} = \int_{4\pi} \rho(\mathbf{n}) n_i n_j \, d\Omega, \tag{12}$$

on the right hand side of eqn (11) is referred to as the damage tensor. In view of eqn (11), the second order tensor approximation of the crack density distribution (5) can be rewritten as:

$$\rho(\mathbf{n}) = \frac{15}{8\pi} D_{ij} n_i n_j - \frac{3\rho_0}{8\pi}. \tag{13}$$

It is instructive to rewrite eqn (13) using the deviatoric part of the damage tensor D_{ij}, defined as:

$$D'_{ij} = \int_{4\pi} \rho(\mathbf{n})(n_i n_j)' \, d\Omega = D_{ij} - \frac{\rho_0}{3} \delta_{ij}, \tag{14}$$

where $(n_i n_j)' = n_i n_j - \frac{1}{3}\delta_{ij}$ is the deviatoric part of the tensor $n_i n_j$. Using eqns (11) and (14) the deviatoric part of the second order crack density tensor is:

$$\rho'_{ij} = \rho_{ij} - \frac{\rho_0}{4\pi} \delta_{ij} = \frac{15}{8\pi} D'_{ij}. \tag{15}$$

Hence, eqns (5) and (13) can be rewritten as:

$$\rho(\mathbf{n}) = \frac{\rho_0}{4\pi} + \frac{15}{8\pi} D'_{ij} n_i n_j. \tag{16}$$

The first term on the right hand side of eqn (16) represents the isotropic damage, defined by a single scalar ρ_0. The second term in eqn (16) represents the second order tensor approximation of the deviation of the crack distribution from its average value.

In the case of two dimensional analysis, the density of all cracks within a unit area is:

$$\rho_0 = \int_{2\pi} \rho(\mathbf{n}) \, d\theta, \tag{17}$$

while the counterparts of eqns (6) and (8) are:

$$\int_{2\pi} n_i n_j \, d\theta = \pi \delta_{ij}, \tag{18}$$

$$\int_{2\pi} n_i n_j n_k n_l \, d\theta = \frac{3\pi}{4} I_{ijkl}. \tag{19}$$

Consequently, the second order approximation of the crack density distribution becomes:

$$\rho(\mathbf{n}) = \frac{2}{\pi} D_{ij} n_i n_j - \frac{\rho_0}{2\pi}, \tag{20}$$

where the second order damage tensor D_{ij} is given by:

$$D_{ij} = \int_{2\pi} \rho(\mathbf{n}) n_i n_j \, d\theta. \tag{21}$$

Equation (20) can be rewritten in terms of the deviatoric part of the damage tensor $D'_{ij} = D_{ij} - \frac{1}{2}\rho_0 \delta_{ij}$ as:

$$\rho(\mathbf{n}) = \frac{\rho_0}{2\pi} + \frac{2}{\pi} D'_{ij} n_i n_j. \tag{22}$$

Again, the last term on the right hand side of eqn (22) represents the deviation from the isotropic damage.

2.3. Fourth order damage tensor

Experimental observations of microcracks in different materials, subjected to a variety of conditions, abound in the existing literature. In general, microcracks are embedded in planes perpendicular to the maximum principal stress. For example, in a material such as rock (Hallbauer et al., 1973; Zheng et al., 1991) subjected to uniaxial compression, the angles subtended by microcrack planes and maximum normal stress are distributed within a range of $\pm(10\text{--}15)°$. The range of angles can be much larger in the case of internal pressures generated by expansive chemical reactions, corrosion, internal heat sources, etc. Higher order tensor variables are, therefore, often needed to improve the accuracy of the approximate (smooth) representation of the complicated crack distribution, generated in the course of arbitrary load programs. The fourth order tensor approximation of the crack density distribution is defined as:

$$\rho(\mathbf{n}) = \rho_{ijkl} n_i n_j n_k n_l, \tag{23}$$

where ρ_{ijkl} are the components of the fourth order crack density tensor. Integrating eqn (23) over all directions n and using eqn (8), it follows that:

$$\rho_{iijj} = \frac{5\rho_0}{4\pi}. \tag{24}$$

The symmetry properties of the crack density tensor, giving $\rho_{iijj} = \rho_{ijij} = \rho_{ijji}$, are utilized in derivation of eqn (24). Furthermore, it can be shown that:

$$\int_{4\pi} n_i n_j n_k n_l n_\alpha n_\beta \, d\Omega = \frac{4\pi}{7} I_{ijkl\alpha\beta}, \tag{25}$$

where

$$I_{ijkl\alpha\beta} = \frac{1}{15}(\delta_{ij} I_{kl\alpha\beta} + \delta_{ik} I_{jl\alpha\beta} + \delta_{il} I_{jk\alpha\beta} + \delta_{i\alpha} I_{jkl\beta} + \delta_{i\beta} I_{jkl\alpha}). \tag{26}$$

The tensor I_{ijkl} in eqn (26) is defined in eqn (9). Multiplying eqn (23) by $n_\alpha n_\beta$ and integrating the product over all directions, leads to:

$$\rho_{iikl} = \frac{35}{16\pi}\left(D_{kl} - \frac{\rho_0}{7}\delta_{kl}\right). \tag{27}$$

It can be similarly shown that:

$$\int_{4\pi} n_i n_j n_k n_l n_\alpha n_\beta n_\gamma n_\delta \, d\Omega = \frac{4\pi}{9} I_{ijkl\alpha\beta\gamma\delta},\tag{28}$$

where:

$$I_{ijkl\alpha\beta\gamma\delta} = \tfrac{1}{105}(\delta_{ij}I_{kl\alpha\beta\gamma\delta}+\delta_{ik}I_{jl\alpha\beta\gamma\delta}+\delta_{il}I_{jk\alpha\beta\gamma\delta}+\delta_{i\alpha}I_{jkl\beta\gamma\delta}+\delta_{i\beta}I_{jkl\alpha\gamma\delta}+\delta_{i\gamma}I_{jkl\alpha\beta\delta}+\delta_{i\delta}I_{jkl\alpha\beta\gamma}).\tag{29}$$

Hence, multiplying eqn (23) by $n_\alpha n_\beta n_\gamma n_\delta$, and integrating the product over the entire solid angle, the fourth order crack density tensor is derived in the following form:

$$\rho_{ijkl} = \frac{315}{32\pi}\left(D_{ijkl}-\frac{2}{3}A_{ijkl}+\frac{\rho_0}{21}I_{ijkl}\right).\tag{30}$$

The fourth order tensor A_{ijkl} in eqn (30) is a sum of the products of the Kronecker delta tensor δ_{ij} and the second order damage tensor D_{ij}, defined in eqn (12), and is given by:

$$A_{ijkl} = \tfrac{1}{6}(\delta_{ij}D_{kl}+\delta_{kl}D_{ij}+\delta_{ik}D_{jl}+\delta_{il}D_{jk}+\delta_{jk}D_{il}+\delta_{jl}D_{ik}).\tag{31}$$

The fourth order damage tensor D_{ijkl}, appearing in eqn (30), is defined by:

$$D_{ijkl} = \int_{4\pi} \rho(n)n_i n_j n_k n_l \, d\Omega.\tag{32}$$

Clearly, any contraction of two indices reduces eqn (32) to the second order damage tensor eqn (12), i.e. $D_{ijkk} = D_{ij}$. Substitution of eqn (30) into eqn (23) leads to the following representation of the crack density distribution:

$$\rho(\mathbf{n}) = \frac{315}{32\pi}D_{ijkl}n_i n_j n_k n_l - \frac{105}{16\pi}D_{ij}n_i n_j + \frac{15\rho_0}{32\pi}.\tag{33}$$

It is instructive to rewrite eqn (33) in terms of the deviatoric parts of the damage tensors. Since the deviatoric part of the product:

$$(n_i n_j n_k n_l)' = n_i n_j n_k n_l - \tfrac{1}{7}(\delta_{ij}n_k n_l+\delta_{kl}n_i n_j+\delta_{ik}n_j n_l+\delta_{il}n_j n_k+\delta_{jk}n_i n_l+\delta_{jl}n_i n_k)+\tfrac{3}{35}I_{ijkl},\tag{34}$$

is defined so that any contraction of its indices gives the zero tensor, it follows that:

$$D'_{ijkl} = \int_{4\pi} (n_i n_j n_k n_l)' \, d\Omega = D_{ijkl}-\frac{6}{7}A_{ijkl}+\frac{3\rho_0}{35}I_{ijkl}.\tag{35}$$

Furthermore, the deviatoric part of the fourth order crack density tensor is:

$$\rho'_{ijkl} = \rho_{ijkl}-\tfrac{1}{7}(\delta_{ij}\rho_{kl\alpha\alpha}+\delta_{kl}\rho_{ij\alpha\alpha}+\delta_{ik}\rho_{jl\alpha\alpha}+\delta_{il}\rho_{jk\alpha\alpha}+\delta_{jk}\rho_{il\alpha\alpha}+\delta_{jl}\rho_{ik\alpha\alpha})+\tfrac{3}{35}\rho_{\alpha\alpha\beta\beta}I_{ijkl}.\tag{36}$$

Hence, in view of eqns (30) and (35),

$$\rho'_{ijkl} = \frac{315}{32\pi}D'_{ijkl}.\tag{37}$$

Introducing eqns (34) and (36) into eqn (23) leads to:

$$\rho(\mathbf{n}) = \rho'_{ijkl}n_in_jn_kn_l + \tfrac{1}{7}(6\rho_{ij\alpha\alpha}n_in_j - \tfrac{11}{35}\rho_{\alpha\alpha\beta\beta}). \tag{38}$$

Since from eqn (27):

$$\rho_{ij\alpha\alpha} = \frac{35}{16\pi}\left(D'_{ij} + \frac{4\rho_0}{21}\delta_{ij}\right), \tag{39}$$

substitution of eqns (24), (37) and (39) into eqn (38) provides an alternate form of the expression (33) for the crack density distribution:

$$\rho(\mathbf{n}) = \frac{\rho_0}{4\pi} + \frac{15}{8\pi}D'_{ij}n_in_j + \frac{315}{32\pi}D'_{ijkl}n_in_jn_kn_l. \tag{40}$$

The first two terms on the right hand side of eqn (40) are identical to the right hand side of the second order approximation, given by expression (16). The last term is, therefore, the refinement associated with the fourth order approximation. Direct comparison between the second and fourth order approximations does not exist when the representations (13) and (33) are utilized. In Kanatani's (1984) paper the various even order damage tensors $D_{ij...}$ are referred to as the fabric tensors of the first kind. The crack density tensors $\rho_{ij...}$ are (within the multiplier of 4π) referred to as the fabric tensors of the second kind. The deviatoric parts of the damage tensors $D'_{ij...}$ are referred to as the fabric tensors of the third kind. More general expressions, involving higher even order tensors, are also available in Kanatani (1984). The related work by Onat and Leckie (1988) contains additional informations related to the representation of damage by even order tensors.

The two dimensional analysis counterparts of the three dimensional expressions (25), (28), (32), (33), (35) and (40), are:

$$\int_{2\pi} n_in_jn_kn_ln_\alpha n_\beta \, \mathrm{d}\theta = \frac{5\pi}{8}I_{ijkl\alpha\beta}, \tag{41}$$

$$\int_{2\pi} n_in_jn_kn_ln_\alpha n_\beta n_\gamma n_\delta \, \mathrm{d}\theta = \frac{35\pi}{64}I_{ijkl\alpha\beta\gamma\delta}, \tag{42}$$

$$D_{ijkl} = \int_{2\pi} \rho(n)n_in_jn_kn_l \, \mathrm{d}\theta, \tag{43}$$

$$\rho(n) = \frac{8}{\pi}D_{ijkl}n_in_jn_kn_l - \frac{6}{\pi}D_{ij}n_in_j + \frac{\rho_0}{2\pi}, \tag{44}$$

$$D'_{ijkl} = D_{ijkl} - A_{ijkl} + \frac{\rho_0}{8}I_{ijkl}, \tag{45}$$

$$\rho(\mathbf{n}) = \frac{\rho_0}{2\pi} + \frac{2}{\pi}D'_{ij}n_in_j + \frac{8}{\pi}D'_{ijkl}n_in_jn_kn_l. \tag{46}$$

Again, the last term on the right hand side of eqn (46) is the refinement of the approximation (22), attributable to the increase in the tensor order.

3. SOME TYPICAL THREE DIMENSIONAL CRACK DISTRIBUTIONS

3.1. *Planar crack distribution*

Consider a family of parallel cracks having identical normal $\mathbf{m} = \{\cos\phi_0\cos\theta_0,$ $\cos\phi_0\sin\theta_0, \sin\phi_0\}$, where ϕ_0 and θ_0 are the spherical angles defining the direction of $\mathbf{m}$.

With $\mathbf{n} = \{\cos\phi\cos\theta,\ \cos\phi\sin\theta,\ \sin\phi\}$ denoting an arbitrary direction, the symmetric form of the crack density distribution is:

$$\rho(\mathbf{n}) = \frac{\rho_0}{2}[\delta(\mathbf{n}-\mathbf{m})+\delta(\mathbf{n}+\mathbf{m})]. \tag{47}$$

This crack configuration is typical of specimens subjected to uniaxial tension. In eqn (47), ρ_0 is the density of all cracks in a unit volume, and δ is the Dirac delta function. Substituting eqn (47) into eqn (12) the second order damage tensor becomes:

$$D_{ij} = \rho_0 m_i m_j. \tag{48}$$

This representation of the damage tensor was extensively utilized in literature (Vakulenko and Kachanov, 1971; Kachanov, 1980; Kachanov 1992). The corresponding second order, continuous approximation of the crack density distribution is derived substituting eqn (48) into eqn (13):

$$\rho(\mathbf{n}) = \frac{3\rho_0}{8\pi}[5(\mathbf{m}\cdot\mathbf{n})^2-1], \tag{49}$$

where ($\cdot$) denotes the scalar product. For example, if $m_i = \delta_{i3}$, eqn (49) becomes:

$$\rho(\phi) = \frac{3\rho_0}{16\pi}(3-5\cos 2\phi). \tag{50}$$

The expression (50) can be rewritten as:

$$\rho(\phi) = \frac{\rho_0}{4\pi} + \frac{5\rho_0}{16\pi}(1-3\cos 2\phi), \tag{51}$$

which corresponds to the crack density representation (16). The first term on the right hand side of eqn (51), i.e. $\rho_0/4\pi$, is the scalar measure of the isotropic approximation of the crack density distribution (47), while the second term represents its second order tensor approximation of the deviation from the isotropy.

The fourth order damage tensor is derived substituting eqn (47) into eqn (32):

$$D_{ijkl} = \rho_0 m_i m_j m_k m_l. \tag{52}$$

Comparing eqn (52) with eqn (48), the relationship between the second and fourth order damage tensors is:

$$D_{ijkl} = \frac{1}{\rho_0}D_{ij}D_{kl}. \tag{53}$$

The fourth order continuous approximation of the crack density distribution (47), is obtained substituting eqns (48) and (52) into eqn (33). This gives:

$$\rho(\mathbf{n}) = \frac{315\rho_0}{32\pi}(\mathbf{m}\cdot\mathbf{n})^4 - \frac{105\rho_0}{16\pi}(\mathbf{m}\cdot\mathbf{n})^2 + \frac{15\rho_0}{32\pi}. \tag{54}$$

For $m_i = \delta_{i3}$, eqn (54) reduces to:

$$\rho(\phi) = \frac{15\rho_0}{256\pi}(15 - 28\cos 2\phi + 21\cos 4\phi). \tag{55}$$

The expression (55) can be rewritten as:

$$\rho(\phi) = \frac{\rho_0}{4\pi} + \frac{5\rho_0}{16\pi}(1 - 3\cos 2\phi) + \frac{9\rho_0}{256\pi}(9 - 20\cos 2\phi + 35\cos 4\phi), \tag{56}$$

which corresponds to the representation (40), of the previous section. The last term on the right hand side of eqn (56) is the fourth order refinement relative to the second order approximation (51).

The graphical representations of the second and fourth order approximate distributions (50) and (55), or (51) and (56), are depicted in Fig. 2. Both distributions have in common the emergence of the negative crack density over a part of the range. In the corresponding regions, the actual cracks are replaced by the stiffening-rigid laminae. These rigid elements are referred to in the literature as negative cracks or anticracks (Dundurs and Markenscoff, 1989). The emergence of negative crack densities during approximations of discontinuous, narrow band width distributions of cracks by continuous distributions provided by tensors should have been expected. Tensorial approximations (50) and (55), of a delta function imply existence of damage at angles other than $\phi = \pi/2$ and $\phi = 3\pi/2$. Consequently, negative crack densities must be present to compensate for this nonexisting damage. Notice
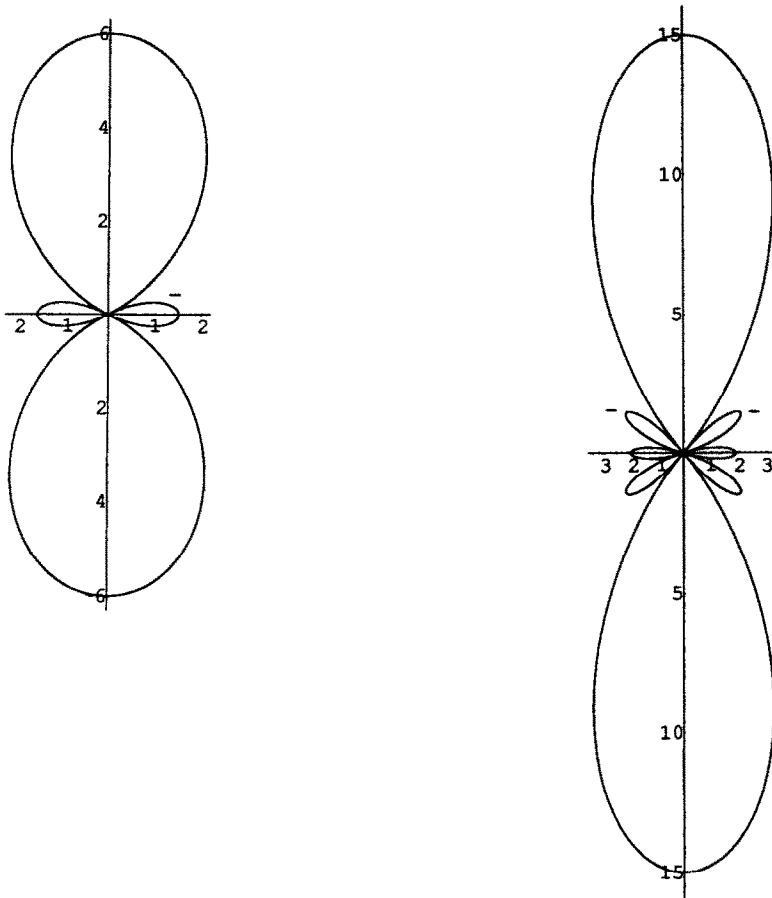

Fig. 2. Second and fourth order tensor approximations of a planar crack distribution. Crack density values are proportional to average crack density. Regions of negative crack density are labeled by negative sign.

that within the second order representation (51), the maximum positive crack density is equal to $6\rho_0/4\pi$, i.e. it is six times greater than the uniform isotropic approximation. The maximum positive crack density of the fourth order representation (56) is $15\rho_0/4\pi$, i.e. 2.5 times greater than that of the second order representation. For example, according to the second order tensor representation only 7.3% of all cracks are located within the range of $(-10°, 10°)$ from the vertical axis. According to the fourth order tensor approximation 17.7% of all cracks are contained within the same range. A closer approximation of the exact (delta) distribution will require introduction of even higher order tensors. The fact that the second order representation predicts more than twice reduced crack density in horizontal planes may have serious consequences on the estimates of effective stiffnesses, onset of localizations, etc. The maximum negative crack density, predicted by eqn (56), occurs in two intersecting families of planes whose normal is defined by $\cos 2\phi = 1/3$, so that $\phi = 35.3°$ and $\phi = 144.7°$. The corresponding crack density is of the magnitude $2.5\rho_0/4\pi$.

3.2. Cylindrical crack distribution

Consider next the system of cracks embedded uniformly in planes parallel to the axis x_3 of the coordinate system x_i ($i = 1, 2, 3$). This case occurs in uniaxial compression of cylindrical specimens. The normal to an arbitrary crack plane is defined as $\mathbf{m} = \{\cos\theta, \sin\theta, 0\}$. This crack distribution is represented by:

$$\rho(\mathbf{n}) = \frac{\rho_0}{2\pi}\delta(\phi),\tag{57}$$

where δ is the Dirac delta function, and $\mathbf{n} = \{\cos\phi\cos\theta, \cos\phi\sin\theta, \sin\phi\}$ is the unit vector defining an arbitrary direction. The scalar multiplier $\rho_0/2\pi$ is introduced so that the total crack density per unit volume is:

$$\int_{4\pi} \rho(\mathbf{n})\,d\Omega = \rho_0.\tag{58}$$

The second order damage tensor is obtained by substituting eqn (57) into eqn (12) and performing requisite integration:

$$D_{ij} = \frac{\rho_0}{2\pi}\int_0^{2\pi} m_i m_j\,d\theta = \frac{\rho_0}{2}(\delta_{ij} - \delta_{i3}\delta_{j3}).\tag{59}$$

The corresponding second order tensor approximation of the crack density distribution (57) follows by inserting eqn (59) into eqn (13):

$$\rho(\phi) = \frac{3\rho_0}{32\pi}(1 + 5\cos 2\phi).\tag{60}$$

This expression can also be cast into the form:

$$\rho(\phi) = \frac{\rho_0}{4\pi} - \frac{5\rho_0}{32\pi}(1 - 3\cos 2\phi),\tag{61}$$

which corresponds to the representation (16) of the previous section. Clearly, the second term on the right hand side of eqn (61) is the second order refinement of the scalar approximation $\rho_0/4\pi$.

The fourth order damage tensor is obtained by substituting eqn (57) into eqn (32):

$$D_{ijkl} = \frac{\rho_0}{2\pi} \int_0^{2\pi} m_i m_j m_k m_l \, d\theta.$$ (62)

Since

$$\int_0^{2\pi} m_i m_j m_k m_l \, d\theta = \frac{\pi}{4} [(\delta_{ij} - \delta_{i3}\delta_{j3})(\delta_{kl} - \delta_{k3}\delta_{l3})$$

$$+ (\delta_{jk} - \delta_{j3}\delta_{k3})(\delta_{il} - \delta_{i3}\delta_{l3}) + (\delta_{ki} - \delta_{k3}\delta_{i3})(\delta_{jl} - \delta_{j3}\delta_{l3})],$$ (63)

the relationship between the second and fourth order damage tensors is:

$$D_{ijkl} = \frac{1}{2\rho_0} (D_{ij}D_{kl} + D_{ik}D_{jl} + D_{il}D_{jk}).$$ (64)

The fourth order continuous crack density approximation is derived by substituting eqns (64) and (59) into eqn (33):

$$\rho(\phi) = \frac{15\rho_0}{2048\pi} (29 + 28\cos 2\phi + 63\cos 4\phi).$$ (65)

The above expression can be rewritten as:

$$\rho(\phi) = \frac{\rho_0}{4\pi} - \frac{5\rho_0}{32\pi} (1 - 3\cos 2\phi) + \frac{27\rho_0}{1048\pi} (9 - 20\cos 2\phi + 35\cos 4\phi),$$ (66)

which is an equivalent representation corresponding to expression (40). The last term on the right hand side of eqn (66) is the fourth order refinement of the second order crack density approximation, given by eqn (61).

The graphs corresponding to distributions (60) and (65), or (61) and (66), are shown in Fig. 3. Maximum crack density according to eqn (60) is 2.25 and according to eqn (65)
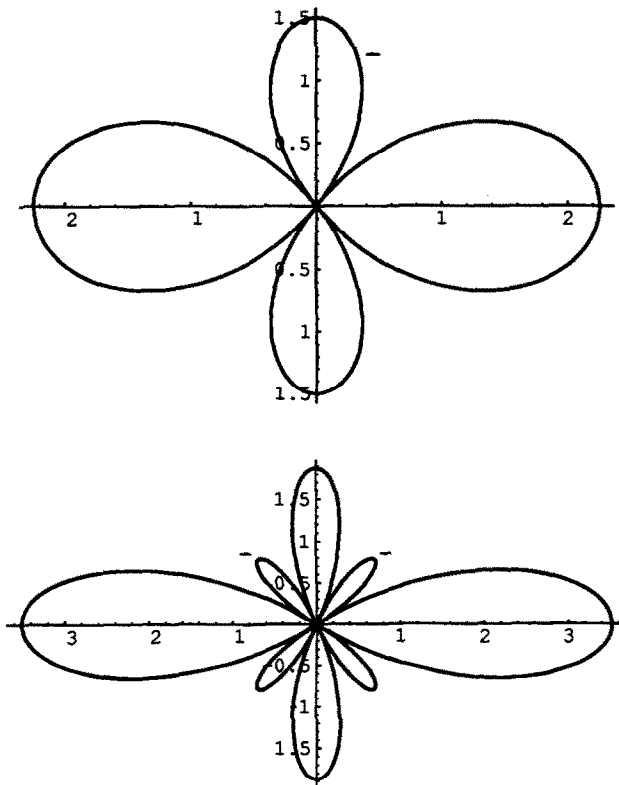

Fig. 3. Second and fourth order tensor approximations of a cylindrical crack distribution. Regions of negative crack density are labeled by negative sign.

3.52 times larger than the isotropic-average value $\rho_0/4\pi$. Within $\pm 10^\circ$ relative to horizontal axis there are 38.4% of all cracks according to eqn (60), and 58.2% according to eqn (65). Closer agreement with the distribution (57) can be achieved with further increase in the order of tensor approximation. In the case of the second order approximation (Fig. 3a), the region of negative crack density (with the maximum magnitude of $1.5\rho_0/4\pi$) is "orthogonal" to the dominating region of positive crack density. The fourth order approximation features two regions of negative crack density, which are at about 45° relative to two "orthogonal" regions of positive cracks. The maximum negative crack density is of the magnitude of $1.04\rho_0/4\pi$, and occurs at the angle defined by $\cos\phi = \pm 2/3$ (i.e. $\phi = 48.2^\circ$ and 131.8°).

4. SOME TYPICAL TWO-DIMENSIONAL CRACK DISTRIBUTIONS

4.1. Parallel cracks

Consider a family of parallel cracks with the area density ρ_0. Let $m = \{\cos\theta_0, \sin\theta_0\}$ be the unit normal to each crack, and let $\mathbf{n} = \{\cos\theta, \sin\theta\}$ be a unit vector defining an arbitrary direction in the plane of cracks. This crack distribution, written in a symmetric form, is:

$$\rho(\mathbf{n}) = \frac{\rho_0}{2}[\delta(\theta-\theta_0)+\delta(\theta-\theta_0-\pi)], \tag{67}$$

where δ is the Dirac delta function. Substitution of eqn (67) into the expression for the second order damage tensor eqn (21) and integrating gives:

$$D_{ij} = \rho_0 m_i m_j. \tag{68}$$

The corresponding second order tensor approximation of eqn (67) is derived by substituting eqn (68) into eqn (20):

$$\rho(\mathbf{n}) = \frac{\rho_0}{2\pi}[4(\mathbf{m}\cdot\mathbf{n})^2 - 1], \tag{69}$$

or, in explicit form as a function of angle θ,

$$\rho(\theta) = \frac{\rho_0}{2\pi} + \frac{\rho_0}{\pi}\cos 2(\theta-\theta_0). \tag{70}$$

The first term on the right hand side of eqn (70), i.e. $\rho_0/2\pi$, is the scalar approximation of the crack density distribution (67), while the second term represents its second order refinement. Maximum positive crack density occurs at angle $\theta = \theta_0$ and is three times greater than the average value $\rho_0/2\pi$, while the maximum negative density occurs at angle $\theta = \theta_0 + \pi/2$ and is of magnitude equal to the average crack density.

The fourth order damage tensor is obtained by introducing eqn (67) into eqn (43):

$$D_{ijkl} = \rho_0 m_i m_j m_k m_l. \tag{71}$$

Substitution of eqns (68) and (71) into eqn (44) now leads to:

$$\rho(\mathbf{n}) = \frac{8\rho_0}{\pi}(\mathbf{m}\cdot\mathbf{n})^4 - \frac{6\rho_0}{\pi}(\mathbf{m}\cdot\mathbf{n})^2 + \frac{\rho_0}{2\pi}, \tag{72}$$

that is,

$$\rho(\theta) = \frac{\rho_0}{2\pi} + \frac{\rho_0}{\pi}\cos 2(\theta - \theta_0) + \frac{\rho_0}{\pi}\cos 4(\theta - \theta_0). \tag{73}$$

The last term on the right hand side of eqn (73) is the fourth order refinement of the second order approximation (70). The graphical representations of distributions (70) and (73) show analogous features to those seen in Fig. 2. The maximum positive crack density according to eqn (73) is five times greater than the average crack density. The maximum negative crack density occurs at the angle defined by $\cos 2(\theta - \theta_0) = -1/4$, and is of the magnitude $1.24\rho_0/2\pi$. According to the second order tensor approximation (70) only 16.4% of all cracks are contained within the planes whose normals are in the range of $\pm 10°$ about the angle $\theta = \theta_0$. The fourth order tensor approximation predicts that 26.6% of all cracks are within this range.

4.2. Two orthogonal systems of cracks

Consider next two mutually orthogonal families of cracks with the respective normals $\mathbf{m} = \{\cos\theta_0, \sin\theta_0\}$ and $\hat{\mathbf{m}} = \{-\sin\theta_0, \cos\theta_0\}$, and crack densities ρ and $\hat{\rho} = \rho_0 - \rho$, where ρ_0 is the total crack density in a unit area. Assume also that $\hat{\rho} = r\rho$, so that:

$$\rho = \frac{1}{1+r}\rho_0, \qquad \hat{\rho} = \frac{r}{1+r}\rho_0. \tag{74}$$

This crack distribution, common to biaxial tension, written in a symmetric form, is:

$$\rho(\theta) = \frac{1}{1+r}\frac{\rho_0}{2}[\delta(\theta - \theta_0) + \delta(\theta - \theta_0 - \pi)] + \frac{r}{1+r}\frac{\rho_0}{2}\left[\delta\left(\theta - \theta_0 - \frac{\pi}{2}\right) + \delta\left(\theta - \theta_0 - \frac{3\pi}{2}\right)\right]. \tag{75}$$

The second order damage tensor is obtained by substituting eqn (75) into eqn (21):

$$D_{ij} = \frac{1}{1+r}\rho_0 m_i m_j + \frac{r}{1+r}\rho_0 \hat{m}_i \hat{m}_j, \tag{76}$$

or, since $m_i m_j + \hat{m}_i \hat{m}_j = \delta_{ij}$,

$$D_{ij} = \frac{1-r}{1+r}\rho_0 m_i m_j + \frac{r}{1+r}\rho_0 \delta_{ij}. \tag{77}$$

The second order continuous approximation of the crack distribution (75) is derived by substituting eqn (77) into eqn (20):

$$\rho(\mathbf{n}) = \frac{1-r}{1+r}\frac{2\rho_0}{\pi}(\mathbf{m}\cdot\mathbf{n})^2 + \frac{3r-1}{1+r}\frac{\rho_0}{2\pi}, \tag{78}$$

that is,

$$\rho(\theta) = \frac{\rho_0}{2\pi} + \frac{1-r}{1+r}\frac{\rho_0}{\pi}\cos 2(\theta - \theta_0). \tag{79}$$

This expression also directly follows by superimposing the two distributions in (70), representing two families of parallel cracks, considered in the previous subsection. Indeed, expression (70) is recovered from eqn (79) by letting $r = 0$. If $r = 1$, from eqn (79) it follows that:

$$\rho(\theta) = \frac{\rho_0}{2\pi}. \tag{80}$$

Thus, according to the second order tensor approximation, two orthogonal crack families with equal crack densities (of $\rho_0/2$ each), are equipolent to the isotropic crack distribution.

The fourth order damage tensor is derived by substituting eqn (75) into eqn (43):

$$D_{ijkl} = \rho_0 m_i m_j m_k m_l + \frac{r}{1+r} \rho_0 (\delta_{ij}\delta_{kl} - \delta_{ij}m_k m_l - m_i m_j \delta_{kl}). \tag{81}$$

Introducing eqn (81) into eqn (44), the expression for the crack density becomes:

$$\rho(\mathbf{n}) = \frac{8\rho_0}{\pi}(\mathbf{m}\cdot\mathbf{n})^4 - \frac{3+5r}{1+r}\frac{2\rho_0}{\pi}(\mathbf{m}\cdot\mathbf{n})^2 + \frac{1+5r}{1+r}\frac{\rho_0}{2\pi}, \tag{82}$$

that is,

$$\rho(\theta) = \frac{\rho_0}{2\pi} + \frac{1-r}{1+r}\frac{\rho_0}{\pi}\cos 2(\theta-\theta_0) + \frac{\rho_0}{\pi}\cos 4(\theta-\theta_0). \tag{83}$$

This expression, again, directly follows from the superposition of the two expressions in eqn (73), recovered from eqn (83) when $r = 0$. The last term on the right hand side of eqn (83) is the fourth order refinement of the second order approximation (79).

If $r = 1$, eqn (83) leads to the corresponding fourth order distribution:

$$\rho(\theta) = \frac{\rho_0}{2\pi} + \frac{\rho_0}{\pi}\cos 4(\theta-\theta_0), \tag{84}$$

so that the fourth order tensor approximation makes a distinction between the isotropic and the considered distribution of cracks. The plots of distributions (80) and (84), approximating two orthogonal crack families of equal densities, are shown in Fig. 4. The second order approximation coincides with the scalar approximation, and is geometrically represented by a circle. The fourth order approximation contains two minor regions of negative crack density, at 45° relative to dominating regions of positive cracks. The maximum crack density, according to the fourth order tensor approximation, is three times larger than the average crack density (scalar and second order tensor approximation).

The approximate crack density distribution does not always contain regions of negative crack density. For example, the presence of these regions in the second order approximation (79) depends on the value of the parameter r. For $\frac{1}{3} \leqslant r \leqslant 3$, the region of negative crack
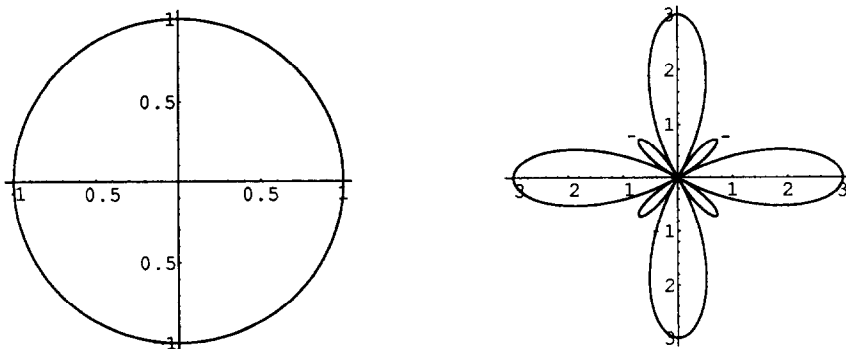

Fig. 4. Second and fourth order tensor approximations of two orthogonal systems of cracks with equal crack densities.
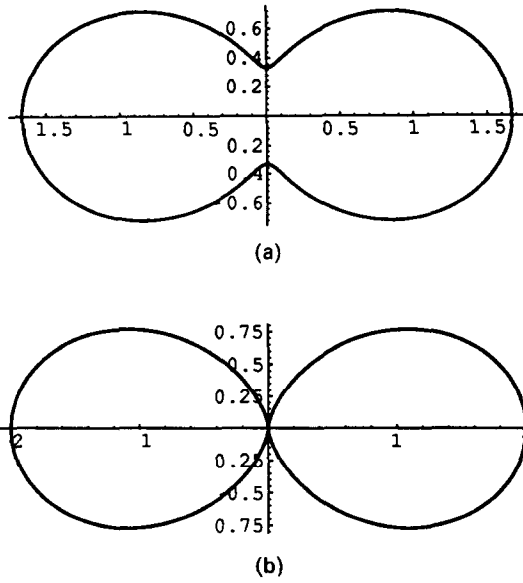
(a)

(b)

Fig. 5. Second order tensor approximation of two orthogonal systems of cracks (a) regions of negative crack density do not occur if one crack density is two times larger than the other, (b) distribution corresponding to the limiting ratio between the crack densities, $r = 3$.

density is absent. The case corresponding to the value $r = 2$ is shown in Fig. 5a. The limiting case corresponding to $r = 3$, at the threshold of the presence of the negative cracks, is shown in Fig. 5b. The other limiting case, corresponding to $r = 1/3$, is obtained from the graph in Fig. 5b through 90° rotation.

4.3. Two nonorthogonal systems of cracks

If the two crack families subtend an arbitrary angle α ("monoclinic" crack distribution), the crack density is:

$$\rho(\theta) = \frac{1}{1+r}\frac{\rho_0}{2}[\delta(\theta-\theta_0)+\delta(\theta-\theta_0-\pi)] + \frac{r}{1+r}\frac{\rho_0}{2}[\delta(\theta-\theta_0-\alpha)+\delta(\theta-\theta_0-\alpha-\pi)].$$

(85)

This case can occur in the case of nonproportional loading, using a procedure analogous to one described in the previous subsection, or superimposing the results derived for a single family of parallel cracks, expressions (70) and (73), the second and fourth order continuous approximations of eqn (85) are derived in the form:

$$\rho(\theta) = \frac{\rho_0}{2\pi} + \frac{1}{1+r}\frac{\rho_0}{\pi}\cos 2(\theta-\theta_0) + \frac{r}{1+r}\frac{\rho_0}{\pi}\cos 2(\theta-\theta_0-\alpha).$$

(86)

$$\rho(\theta) = \frac{\rho_0}{2\pi} + \frac{1}{1+r}\frac{\rho_0}{\pi}\cos 2(\theta-\theta_0) + \frac{1}{1+r}\frac{\rho_0}{\pi}\cos 4(\theta-\theta_0)$$

$$+ \frac{r}{1+r}\frac{\rho_0}{\pi}\cos 2(\theta-\theta_0-\alpha) + \frac{r}{1+r}\frac{\rho_0}{\pi}\cos 4(\theta-\theta_0-\alpha). \quad (87)$$

Clearly, if $r = 0$ eqns (86) and (87) reduce to eqns (70) and (73). If $\alpha = \pi/2$, the results
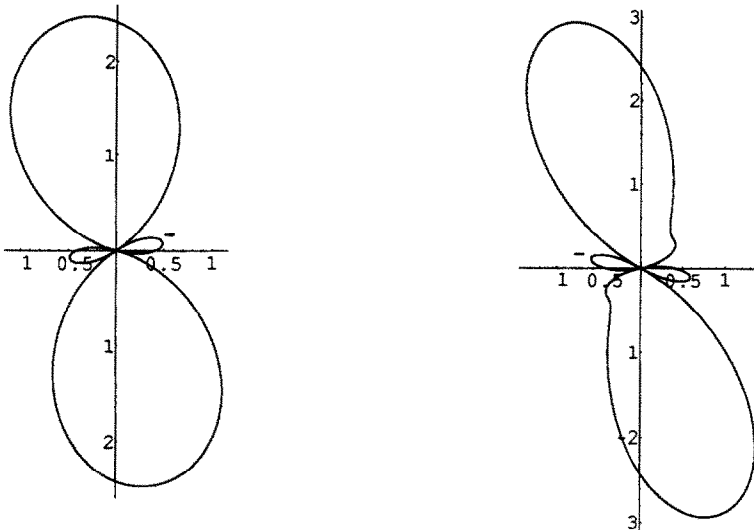
Fig. 6. Second and fourth order tensor approximations of two nonorthogonal systems of cracks.
Angle between the crack planes is $\pi/4$, and the density of one crack system is two times larger than
the other.

eqns (79) and (83) for two orthogonal crack families are recovered. Figure 6 displays the
graphs of the approximate crack density representations (86) and (87), for the case when
two crack families subtend the angle $\alpha = \pi/4$, and the density of one family is twice as large
as the density of the other, i.e. $r = 2$. The angle θ_0 is taken to be $3\pi/8$, such that two families
are symmetrically positioned with respect to the vertical axis. Note that the graph in Fig.
6a, obtained from the nonorthogonal crack family solution (86), can also be obtained from
the orthogonal crack family solution (79), by adjusting its densities and orientations as the
eigenvalues and eigendirections of the second order damage tensor:

$$D_{ij} = \frac{1}{1+r}\rho_0 m_i m_j + \frac{r}{1+r}\rho_0 \hat{m}_i \hat{m}_j. \tag{88}$$

In eqn (88), $\mathbf{m} = \{\cos\theta_0, \sin\theta_0\}$ and $\hat{\mathbf{m}} = \{\cos(\theta_0+\alpha), \sin(\theta_0+\alpha)\}$. The planes of
maximum crack densities of the actual distribution naturally differ from these principal
planes of the second order tensor. Hence, in the case of the monoclinic crack distribution
the second order tensor approximation becomes less adequate, both in terms of principal
densities and their orientations.

4.4 Rosette histogram

Consider finally the crack distribution measured in actual tests. For example, Fig. 7
shows a rosette histogram deduced from the measurements of microcrack orientation and
density in quartzite specimen tested in triaxial compression machine (Hallbauer *et al.*,
1973). The majority of cracks were oriented within $\pm 10°$ to the longitudinal axis of the
specimen. The experimental data is approximately represented by a rosette histogram in
which cracks are distributed between the angles of 70–95°. The crack densities in five
subregions, each spanning the angle of 5°, are 1.8, 7.2, 10.8, 14.4 and 1.8 times the average
crack density $\rho_0/2\pi$. The rosette histogram has a central symmetry, so that the crack density
in an arbitrary direction $\mathbf{n}$ is equal to that in the direction $-\mathbf{n}$.

The corresponding second order damage tensor is obtained by substituting the crack
distribution $\rho(\mathbf{n})$ from the rosette histogram in Fig. 7 into the expression (21). Performing
requisite integration, it follows that $D_{11} = 0.385$, $D_{22} = 5.897$ and $D_{12} = D_{21} = 0.695$ times
the average crack density $\rho_0/2\pi$. Substituting these components into eqn (20), the second
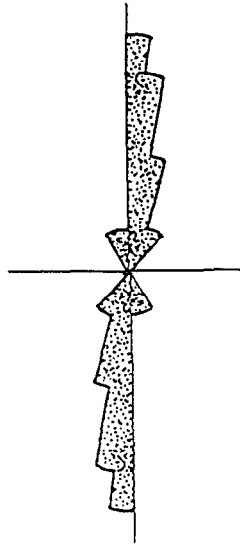order tensor approximation of the rosette histogram crack distribution is:

Fig. 7. Rosette histogram deduced from the measurements of crack distribution in triaxial compression of quartzite specimen (Hallbauer et al., 1973).

$$\rho(\theta) = \frac{\rho_0}{2\pi}(1 - 1.755\cos 2\theta + 0.442\sin 2\theta).\tag{89}$$

The graph of the distribution (89) is shown in Fig. 8a. The maximum positive crack density is 2.81 times the average crack density, and occurs at angle $\theta = 83°$. The maximum negative crack density is 0.81 times the average crack density, and occurs at angle $\theta = -7°$.

To derive the fourth order tensor approximation of the rosette histogram crack distribution, the components of the fourth order damage tensor (43) are first evaluated. It follows that $D_{1111} = 0.263$, $D_{2222} = 5.775$, $D_{1122} = 0.122$, $D_{1112} = 0.026$ and $D_{2221} = 0.669$ times the average crack density $\rho_0/2\pi$. The symmetry properties define the values of other components: $D_{1122} = D_{2211} = D_{1221} = D_{2112}$, $D_{1112} = D_{1121} = D_{1211} = D_{2111}$ and $D_{2221} = D_{2212} = D_{2122} = D_{1222}$. Substitution into eqn (44), therefore, gives:
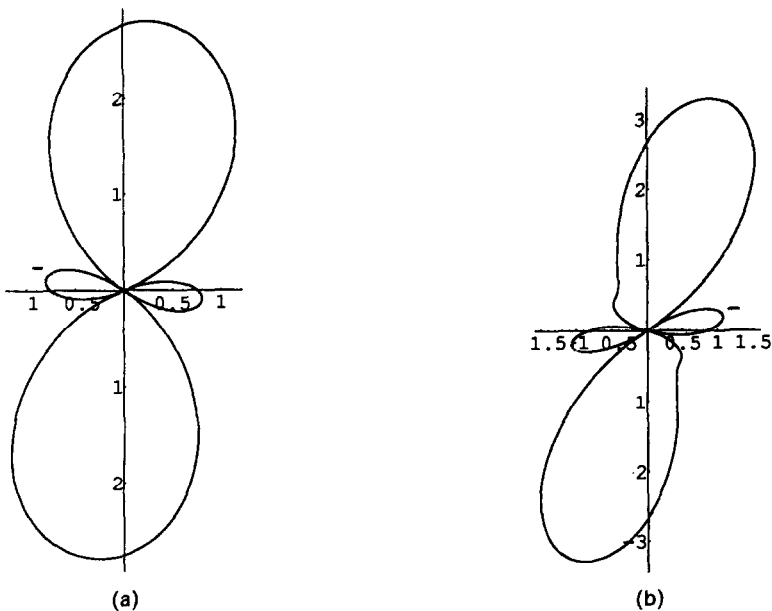

(a)   (b)

Fig. 8. (a) Second, and (b) fourth order tensor approximations of the rosette histogram from Fig. 7.

$$\rho(\theta) = \frac{\rho_0}{2\pi}(1 - 1.755\cos 2\theta + 0.442\sin 2\theta - 0.086\cos 4\theta - 0.820\sin 4\theta). \qquad (90)$$

The first three terms in the right hand side of eqn (90) are exactly equal to those of the second order tensor approximation (89), while the last two terms represent the refinement of the continuous approximation due to the fourth order damage tensor. The graph of the distribution (90) is depicted in Fig. 8b. According to this distribution, 42% of all cracks are distributed within the angle range of 70–95° and 250–275° (the range of nonzero crack distribution of the rosette histogram in Fig. 7). The maximum positive crack density is 3.43 times the average crack density, and occurs at the angle $\theta = 72°$. The maximum negative crack density is of the magnitude 1.09 times the average crack density, and occurs at the angle $\theta = 11°$. Much better reproduction of the rosette histogram crack distribution is evident, both with respect to the orientation and the density of cracks.

5. CONCLUDING REMARKS

Formulation of continuum damage theories requires approximation of discontinuous and often nondeterministic distribution of cracks by continuous functions computed from a sequence of even order tensors. Even though approximations by even order tensors were extensively used in the past, their accuracy was never seriously examined. The main objective of this study is to establish a relationship between the experimental measurements (rosette histograms) of crack density distribution and the continuous representations provided by scalar, second order tensor and fourth order tensor damage parameters. The accomplishment of this task will provide the means to estimate the accuracy of various tensorial representations.

The analysis of several frequently encountered crack distributions, corresponding to uniaxial and biaxial stress fields, clearly indicates the shortcomings of the scalar and second order tensor approximations. In all examined cases the fourth order tensor provided superior, if not always satisfactory, estimates of crack distributions. This was especially obvious for the monoclinic crack distribution. A common feature that arises in many cases, when either second or fourth order damage tensors are utilized to obtain the approximate continuous distribution, is the occurrence of regions with negative crack density ("anti-crack" regions).

All examined approximations were not entirely satisfactory in dealing with crack systems distributed within a small band of orientations. This is, naturally of some concern since the macro-failure, according to the percolation theory (Krajcinovic et al., 1992), strongly depends on the density and orientation of cracks. Moreover, the second order tensor representation does not make a distinction between the random and orthogonal distribution of cracks. However, as shown in Balberg (1985), the critical crack densities in these two cases are not identical.

It should also be pointed out that in the literature the damage tensor is often introduced phenomenologically, through its relationship with the so called effective stress operator (Ju, 1989; Chaboche, 1992). Actual analysis of the relation between suggested representations and considered crack distributions was, however, not attempted. As a result, the existence of "anticracks" was never contemplated. More importantly, the influence of the "anti-cracks" on the macro response was not discussed in the existing literature, providing an important subject for future research.

REFERENCES

Balberg, I. (1985). "Universal" percolation-threshold limits in the continuum. *Phys. Rev. B* **31**, 4053–4055.
Chaboche, J. L. (1982). Le concept de contrainte effective, appliqué à l'élasticité et à la viscoplasticité en présence d'un endommagement anisotroppe. In *Mechanical behavior of anisotropic solids, Proc. Euromech Col., 115, June 1979* (Edited by J. P. Boehler), pp. 737–760, Martinus Nijhoff, The Netherlands.

Chaboche, J. L. (1992). Damage induced anisotropy: on the difficulties associated with the active/passive unilateral condition. *Int. J. Damage Mech.* **1**, 148–171.

Chow, C. L. and Wang, J. (1988). Ductile fracture characterization with an anisotropic continuum damage theory. *Engng Fracture Mech.* **30**, 547–563.

Cordebois, J. P. and Sidoroff, F. (1982). Endommagement anisotrope en élasticité et plasticité. *J. Mécanique théorique et appliquée*, Numéro spécial, 45–60.

Davison, L. and Stevens, A. L. (1973). Thermodynamic constitution of spalling elastic bodies. *J. Appl. Phys.* **44**, 668–674.

Dragon, A. and Mroz, Z. (1979). A continuum model for plastic brittle behavior of rock and concrete. *Int. J. Eng. Sci.* **17**, 121–137.

Dundurs, J. and Markenscoff, X. (1989). A Green's function formulation of anticracks and their interaction with load-induced singularities. *J. Appl. Mech.* **56**, 550–555.

Hallbauer, D. K., Wagner, H. and Cook, N. G. W. (1973). Some observations concerning the microscopic and mechanical behavior of quartzite specimens in stiff, triaxial compression tests. *Int. J. Rock Mech. Sci. Geomech. Abstr.* **10**, 713–726.

Ju, J. W. (1989). On energy-based coupled elastoplastic damage theories: constitutive modeling and computational aspects. *Int. J. Solids Structs* **25**, 803–833.

Kachanov, L. M. (1958). On the creep rupture time. *Izv. AN SSSR, Otd. Tekhn. Nauk* **8**, 26–31.

Kachanov, M. (1980). Continuum model of medium with cracks. *J. Engng Mech. Div.* **106**, 1039–1051.

Kachanov, M. (1992). Effective elastic properties of cracked solids: critical review of some basic concepts. *Appl. Mech. Rev.* **45**, 304–335.

Kanatani, K. (1984). Distribution of directional data and fabric tensors. *Int. J. Engng Sci.* **22**, 149–164.

Karihaloo, B. L. and Fu, D. (1989). A damage-based constitutive law for plain concrete in tension. *Eur. J. Mech. A/Solids* **8**, 373–384.

Krajcinovic, D. (1989). Damage mechanics. *Mech. Mater.* **8**, 117–197.

Krajcinovic, D. and Fonseka, G. U. (1981). The continuous damage theory of brittle materials. *J. Appl. Mech.* **48**, 809 815.

Krajcinovic, D., Sumarac, D. and Mallick, K. (1992). Elastic parameters of brittle elastic solids containing slits—critical state. *Int. J. Damage Mech.* **1**, 386–403.

Lemaitre, J. (1987). Formulation and identification of damage kinetic constitutive equations. In *Continuum Damage Mechanics—Theory and Application* (Edited by D. Krajcinovic and J. Lemaitre), CISM courses and lectures no. 295, pp. 37–89, Springer-Verlag, Wien.

Lemaitre, J. (1992). *A Course on Damage Mechanics*. Springer-Verlag, Berlin.

Lemaitre, J. and Chaboche, J. L. (1978). Aspect phenomenologique de la rapture par endommagement. *J. de Mécanique appliquée* **2**, 317–365.

Lubarda, V. A. and Krajcinovic, D. (1993). Tensorial representation of the effective elastic properties of the damaged material. *Int. J. Damage Mech.* (In press).

Murakami, S. (1988). Mechanical modeling of material damage. *J. Appl. Mech.* **55**, 280–286.

Onat, E. T. and Leckie, F. A. (1988). Representation of mechanical behavior in the presence of changing internal structure. *J. Appl. Mech.* **55**, 1–10.

Simo, J. C. and Ju, J. W. (1987). Strain and stress based continuum damage models—I. Formulation. *Int. J. Solids Structs* **23**, 821–840.

Talreja, R. (1985). A continuum mechanics characterization of damage in composite materials. *Proc. R. Soc. London A* **399**, 195–216.

Vakulenko, A. A. and Kachanov, M. L. (1971). Continuum model of medium with cracks. *Mekhanika Tverdogo Tela* **4**, 159–166 (in Russian).

Zheng, Z., McLennan, J. and Martin, W. (1991). Compressive stress-induced microcracks and effective elastic properties of limestone and concrete. Phase I final technical report, submitted to AFOSR/XOT by Terra Tek, Inc.